FUNDAMENTAL FREQUENCY APPROXIMATION FOR THE PHASE OF A RESONANT LOAD

Selçuk Kılınç Özlem Öztürk Haldun Karaca
e-mail: selcuk.kilinc@eee.deu.edu.tr; ozlem.ozturk@eee.deu.edu.tr; haldun.karaca@deu.edu.tr
Dokuz Eylül University, Engineering Faculty, Department of Electrical and Electronics Engineering, Kaynaklar Campus, 35160, Buca, İzmir, Turkey

Key words: resonant load, modeling, sinusoidal steady-state analysis, fundamental frequency approximation

ABSTRACT

In this study, the validity of the approximation used in the modeling of resonant inverter tuning loop is discussed. With this approach, the phase-frequency relation of a resonant load around load resonant frequency can be expressed as a linear function for a reasonably high quality factor load. Results are verified by simulations.

I. INTRODUCTION

The steady-state analysis of resonant inverters (RIs), or at least a part of it, is usually done by assuming that its load is driven by a sinusoidal voltage (for series RI) or sinusoidal current (for parallel RI). In fact, the load is excited by a square-wave current or square-wave voltage in a parallel inverter or series inverter, respectively. The response of a load with a reasonable Q factor (for instance Q≥2) to a square-wave driving would be nearly a sinusoidal waveform when excitation frequency f is about at its resonant frequency f_r. It is well known that the band-pass characteristics of the resonant load around f_r and large attenuation at the harmonic frequencies lead to this behavior of the load. It can be easily shown that this approach gives more acceptable results when f gets more close to f_r and Q of the load increases. This well-known simplification is used in this study to characterize the phase of the load with a simple yet acceptable expression. In this paper, this approach will be examined theoretically and visualized by using several plots.

II. MODEL OF RESONANT INVERTER TUNING LOOP WITH VOLTAGE-OUTPUT CHARGE-PUMP PHASE-FREQUENCY DETECTOR

RIs are mostly used as supplies for induction heating and ultrasonic motor driving applications [1]. Ultrasonic measurements sometimes require an RI for the excitation of a resonant transducer at one of its resonant frequencies [2]. Since the power switches in RIs are operated at either zero voltage condition (parallel inverter) or zero current condition (series inverter), switching losses are normally less than that of the other inverter types [1]. In order to maintain zero voltage or zero current switching conditions against the load parameter variations, a frequency control circuitry is required in an RI. Phase-locked-loop (PLL) technique is commonly used for this purpose [3]. This loop adjusts operating frequency (f) of the RI by forcing the phase difference between load current and load voltage to be zero. This is the ultimate goal of the control loop and when it is achieved f becomes equal to the load resonant frequency (f_r).

Charge-pump phase-frequency detector (CP/PFD) offers some advantages over other types of phase detectors for tuning loop of RIs. Utilization of a CP/PFD, disregarding voltage or current output type, in the tuning loop of an RI eliminates the necessity of an integrator circuit while loops having a phase detector without tri-state property require an integrator circuit for zero steady state phase error [2]. A diagram of a tuning loop, which uses a CP/PFD, is shown in Figure 1. Operating frequency of an RI is produced by the voltage-controlled oscillator (VCO) in this scheme. In the tuned condition, output of the CP/PFD remains continuously at its open circuit state and filter preserves correct voltage value to drive the load at f_r through the VCO. Some commercially available PLL chips such as well known MC14046B [4], which is frequently employed in RI applications, contain a voltage output CP/PFD rather than a CP/PFD with well-known output property. Therefore, a behavioral modeling can be useful for the design of frequency control loops which employ voltage output CP/PFD and may provide a deep insight into the operation of these loops.

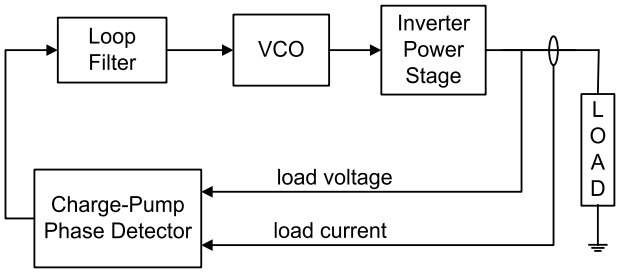

Figure 1. Simplified scheme of an RI tuning loop

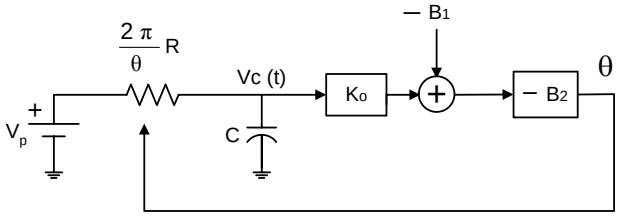

Figure 2. The model for tuning loop with a voltage output CP/PFD and simple RC filter for θ > 0

Figure 2 depicts the model for RI tuning loops that contain CP/PFD. This model is proposed in our early work [5] for positive θ values. The detailed analysis and the experimental confirmation of the model are presented in [5]. It uses the fundamental frequency approximation for behavior of resonant load. This approximation yields that a resonant load with a reasonable Q can be characterized as a constant. In the following, the derivation of this approximation is given.

III. FUNDAMENTAL FREQUENCY APPROXIMATION

The following analysis uses frequency values normalized to ω_r (angular resonant frequency) for the purpose of generality. Let a series resonant load shown in Figure 3 be excited by a square-wave voltage source with an angular frequency of ω around ω_r. Let us define $\Omega = \omega/\omega_r$ as the normalized source frequency. Since the excitation signal is composed of various harmonics then for the n[th] harmonic, the impedance presented by the load to this harmonic component of the source $Z_n(\omega)$ can be expressed as

$$Z_n(\omega) = Z(n\omega) = j(n\omega)L_s + \frac{1}{j(n\omega)C_s} + R_s \quad (1)$$

Using the normalized frequency Ω value, the above expression becomes

$$Z_n(\Omega\omega_r) = Z_n(\omega) = j(n\Omega\omega_r)L_s + \frac{1}{j(n\Omega\omega_r)C_s} + R_s \quad (2)$$

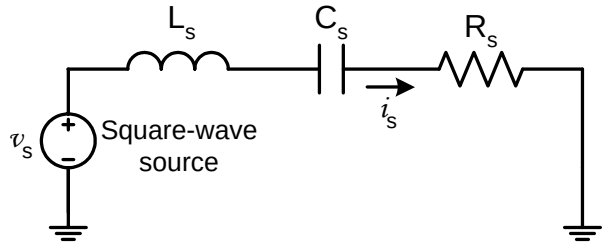

Figure 3. The circuit demonstrating fundamental frequency approximation

From the circuit theory, we can write the nth harmonic phasor as of i_s as

$$I_n(\Omega\omega_r) = \frac{V_n(\Omega\omega_r)}{Z_n(\Omega\omega_r)} \quad (3)$$

Here V_n is the n[th] harmonic content of the source v_s and similarly I_n denotes the n[th] harmonic phasor of the current in Figure 3. Defining the n[th] harmonic admittance $Y(n\Omega\omega_r)$ as

$$Y(n\Omega\omega_r) = Y_n(\Omega\omega_r) = 1/Z_n(\Omega\omega_r) \quad (4)$$

and, in terms of harmonic admittance, (3) can be rewritten as

$$I_n(\Omega\omega_r) = V_n(\Omega\omega_r) \cdot Y_n(\Omega\omega_r) \quad (5)$$

Remembering that the Q factor of the load in Figure 3 is

$$Q = 1/\omega_r R_s C_s \quad (6)$$

By combining (6) with (1) and (4), $Y_n(\Omega\omega_r)$ can be expressed as

$$Y_n(\Omega\omega_r) = \frac{j(n\Omega)\omega_r C_s}{\left[1-(n\Omega)^2\right] + jn\Omega\frac{1}{Q}} \quad (7)$$

where $\omega_r = \sqrt{\frac{1}{L_s C_s}}$.

In the following analysis Q is assumed to be known and the square-wave driving signal has a transition at t=0 thus it consists of only odd harmonics magnitudes of which are decreasing with proportional to 1/n. This way, the i_s current of Figure 3 can be expressed from (5) as below

$$i_s(t) = \sum_{n=1,3,5}^{\infty} \frac{1}{n}\left|Y_n(\Omega\omega_r)\right| \sin\left[(n\Omega\omega_r)t + \angle Y_n(\Omega\omega_r)\right] \quad (8)$$

For simplicity, the square-wave fundamental magnitude is assumed to be unity. Since it is not possible to deal with infinite number of harmonics numerically, a limit is needed to be taken on n, which is selected here as 49. Then we can write for $i_s(t)$

$$i_s(t) \cong \sum_{n=1,3,5}^{49} \frac{1}{n}\left|Y_n(\Omega\omega_r)\right|\sin\left[(n\Omega\omega_r)t + \angle Y_n(\Omega\omega_r)\right] \tag{9}$$

To get the phase of $i_s(t)$ referenced to $v_s(t)$, the solution of $i_s(t)=0$ around t=0 should be found. Using (9), we can write

$$i_s(t) = \sum_{n=1,3,5}^{49} \frac{1}{n}\left|Y_n(\Omega\omega_r)\right|\sin\left[(n\Omega\omega_r)t + \angle Y_n(\Omega)\omega_r\right] = 0 \tag{10}$$

A close look into (10) reveals that taking $\omega_r C_s = 1$ in (7) will not alter the solutions of the t values, which satisfy this equation. Input source, on the other hand, is assumed to have a zero crossing at t=0, therefore one of the solutions of $i_s(t) = 0$, say t_1, is directly related to the phase of $i_s(t)$. From among the solutions of (10), let us denote the one with the minimum absolute value as t_1. If we could determine this t_1, then we can calculate the phase of the resonant load current from it. This is due to the fact that the phase of the current in a series resonance circuit is less than $|\pi/2|$ rad when driven by a periodic source signal. Inserting $\theta = \omega t_1 = \Omega\omega_r t_1$ (here θ is the phase of $i_s(t)$), if we rewrite (10) in terms of θ then we obtain

$$i_s(t_1) = \sum_{n=1,3,5}^{49} \frac{1}{n}\left|Y_n(\Omega\omega_r)\right|\sin\left[(n\theta) + \angle Y_n(\Omega\omega_r)\right] = 0 \tag{11}$$

The phase of θ could be calculated from this equation for any normalized frequency Ω if ω_r and C_s are known and placed into (7). However an examination of (7) and (11) reveals that an assumption of $\omega_r = 1$ and $C_s = 1$ would never alter θ against Ω characteristic defined implicitly by (11).

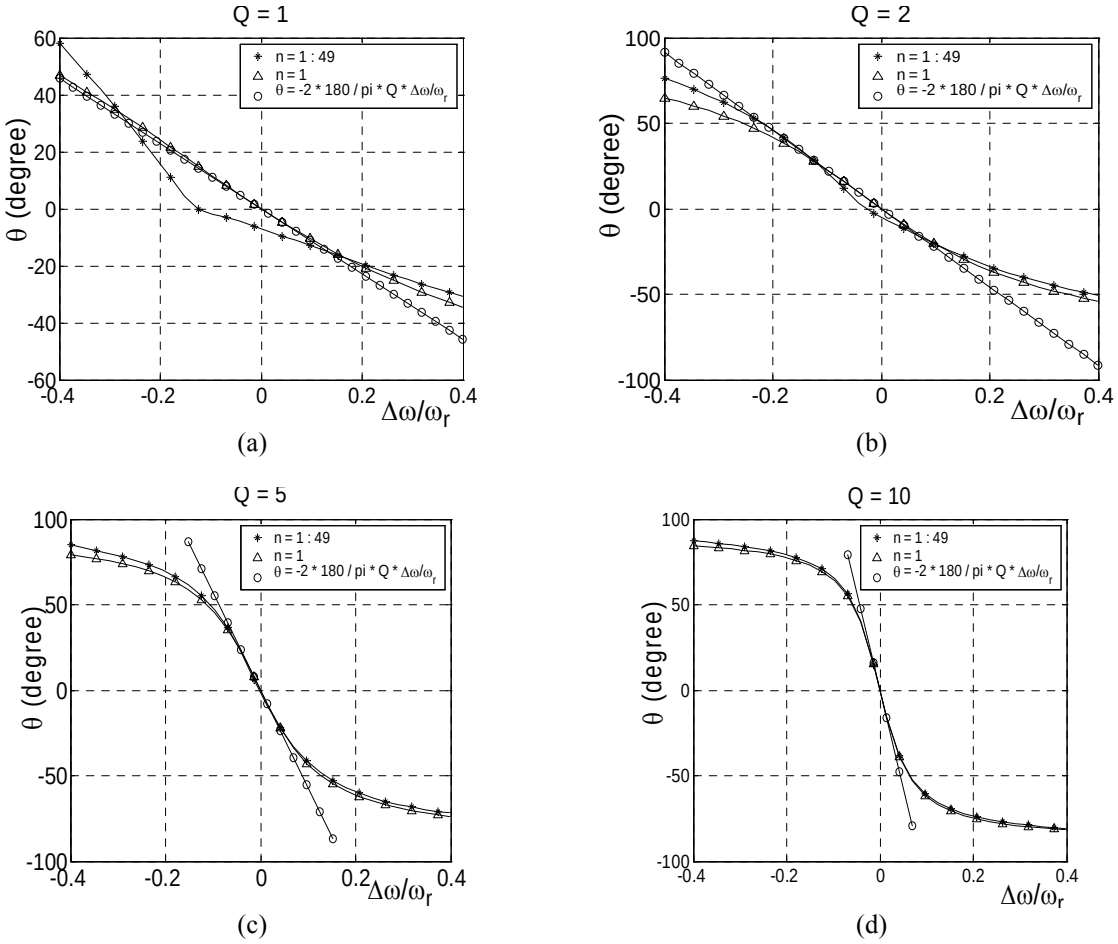

Figure 4. Current phase against frequency curves of a series resonant circuit obtained using three different approximations: (a) Q=1, (b) Q=2, (c) Q=5, (d) Q=10; Δ: square wave driving approximated by using fundamental and upto 49th harmonics, *: fundamental frequency approximation (FFA), o: approximated characteristics for FFA

IV. SIMULATION RESULTS

A MATLAB routine (see Appendix), which calculates θ as absolute minimum for a given Ω, is written to verify the phase approximation used in this paper. In this routine, load Q is given as a parameter and it calculates phase against normalized frequency characteristics. For a better interpretation of these characteristics, the plots given in Figure 4 are arranged in such a way that they use axis parameter (Ω-1) or $\Delta\omega/\omega_r$ rather than Ω. Three curves against $\Delta\omega/\omega_r$ are introduced in each plot. One of them is obtained as just described in this Appendix taking into account source harmonics up to 49th, while the second is obtained by assuming that v_s in Figure 3 is a sinusoidal source (Fundamental Frequency Approximation). The third characteristic given in each plot is a tangent line to that of the second characteristic obtained assuming a sinusoidal source. In this paper, the phase characteristic of a resonant load is expressed with the equation

$$\theta = -2Q(\Delta\omega/\omega_r) \tag{12}$$

which is the slope of above tangent line. Note that this phase approximation is obtained by applying two approximations sequentially. The plots given for Q=1, Q=2, Q=5, and Q=10 values clearly indicate that (12) is a good approximation for the phase of a load for reasonable Q values such as Q≥2.

Similarly, the voltage phase versus $\Delta\omega/\omega_r$ characteristics could be obtained for a parallel resonant load driven from a square-wave current source. With a little work it can be seen that the phase versus frequency characteristics of the series and parallel resonant loads are exactly the same. The only difference is that in the case of parallel resonant load, θ represents the phase of the load voltage with reference to its driving current source. Therefore the analysis introduced in this paper, which uses the approximation $\theta = -2Q(\Delta\omega/\omega_r)$, is equally applicable to both the series and parallel resonant loads. The only difference is that in a parallel RI θ is the phase of the load voltage referenced to its current excitation form because of the fact that in practice parallel resonant loads are driven by a current source.

V. DISCUSSION

It is observed that the plots in Figure 4 produce confusing results after a certain value of $\Delta\omega/\omega_r$ beyond well above the limit of ±0.4 taken in this study, which depends on Q. For example, the value of θ calculated for an excitation which includes all the harmonics of a square wave up to the 49th one, e.g. $\Delta\omega/\omega_r$ =0.6 and Q=10, is observed to be very different from the θ plot which would be obtained for the same parameters of the sinusoidal excitation. This is due to the fact that the excitation frequency in this situation becomes different from the frequency of load current (for a series resonant load) or the frequency of the load voltage (for a parallel resonant load) and it cannot be mentioned about a phase difference. It results in a complex but periodic signal at a frequency that is three times of the load driving frequency. For instance, third harmonic of the current in a series resonant load dominates and frequency of the current becomes three times of the excitation.

The behavior of the tuning loop in such a case could be very different depending on the type of the phase detector in the loop. For example, since a PFD could also detect the difference in frequency, the tuning could be achieved by steering the loop frequency in the correct direction in the case of a loop, which uses this PFD. On the other hand, if a multiplier type phase detector is used in a loop, then the loop could have null frequencies other than the ω_r frequency and the tuning could not be achieved by the loop. This situation is similar to the mechanism encountered in PLL circuits using PFD where there is no harmonic locking and to the mechanism seen in PLL circuits using multiplier phase detector in which there is a disadvantage of harmonic locking.

VI. CONCLUSION

The applicability of fundamental frequency approximation in the phase of resonant load is discussed. This approximation was previously used in the model of RI tuning loops that employ voltage-output CP/PFD [5] without its derivation. Here we give its analysis and verification in detail. As a result of this approximation, it is concluded that the phase of a resonant load with a reasonable Q can be characterized as a constant around its resonant frequency. Derived plots show that the approximation will give acceptable results for a Q value between 1 and 10.

REFERENCES

1. A. Schönknecht and R.W.A.A. De Doncker, “Novel topology for parallel connection of soft-switching high-power high-frequency inverters”, IEEE Transactions on Industry Applications, vol. 39, no. 2, pp. 550-555, 2003.
2. V. Ferrari, D. Marioli and A. Taroni, “Improving the accuracy and operating range of quartz microbalance sensors by a purposely designed oscillator circuit”, IEEE Transactions on Instrumentation and Measurement, vol. 50, no. 5, pp. 1119-1122, 2001.
3. H. Karaca, A.K. Tanç and S. Kılınç, “Analysis of tuning in resonant inverter”, Electronics Letters, vol. 38, no. 20, pp. 1155-1156, 2002.
4. MC14046B CMOS Micropower Phase Locked Loop Data Sheet, CMOS Logic Data Book, DL131/D, Motorola Semiconductor, pp. 6.120-6.124, 1991.
5. S. Kılınç, H. Karaca, A New Model for Voltage Output Charge-Pump Phase Frequency Detector in Resonant Inverter Tuning Loops, IEEE International Midwest Symposium on Circuits and Systems, II, 301-304, Jul., 2004, Hiroshima, Japan.

APPENDIX

NOTE: The Q (Quality Factor) of the load should be given at the 10th row of the program as Q = number. This value is selected as 5 as a default value in the following code.

```
%   Y(n) = i*n*omega / ((1-n^2*omega^2)+i*(n*omega/Q))
%
% and
%
%   Ut = sum(1/n*abs(Y(n))*sin(-n*teta+Y(n)))
%
% Problem : Find theta that minimizes Ut.
%
clear;clc;close('all');
Q=5;
omega=linspace(0.6,1.4,30);
n=1:2:50;
n1=1;
theta=-pi/2:.001:pi/2;
for j=1:length(theta)
    for k=1:length(omega)
        Y=i*n*omega(k)./((1-n.^2*omega(k)^2)+i*(n*omega(k)/Q));
        Y1=i*n1*omega(k)./((1-n1.^2*omega(k)^2)+i*(n1*omega(k)/Q));
        U(j,k)=sum(1./n.*abs(Y).*sin(-n*theta(j)+angle(Y)));
        U1(j,k)=sum(1./n1.*abs(Y1).*sin(-n1*theta(j)+angle(Y1)));
    end

end

for m=1:30,
    f(m)=theta(find(abs(U(:,m))==min(abs(U(:,m)))))*180/pi;
    f1(m)=theta(find(abs(U1(:,m))==min(abs(U1(:,m)))))*180/pi;
end
model = -2*Q*(omega-1)*180/pi;
ind_model = find(model <= 100 & model >= -100);
ind_omega = find(omega >= 0.85 & omega < 1.15);
figure;
axes('Box','on');
hold on;
title(['\fontsize{14}' 'Q = ' num2str(Q)]);
plot(omega(1:2:end)-1,f(1:2:end),'k*',omega(1:2:end)-
1,f1(1:2:end),'k^',omega(ind_model)-1,model(ind_model),'ko');



legend('\fontsize{10}n = 1 : 49','\fontsize{10}n = 1', ['\fontsize{10}' '\theta'
' =
-2 * 180 / pi * Q * ' '\Delta\omega/\omega_r']);
plot(omega-1,f,'k-',omega-1,f1,'k-',omega(ind_model)-1,model(ind_model),'k-');
xlabel('\fontsize{14}\Delta\omega/\omega_r');
ylabel('\fontsize{16}\theta \fontsize{14}(degree)');
grid;
```